Microchimica Acta (2018) 185: 259
https://doi.org/10.1007/s00604-018-2811-9

ORIGINAL PAPER

Exonuclease-assisted multicolor aptasensor for visual detection of ochratoxin A based on G-quadruplex-hemin DNAzyme-mediated etching of gold nanorod

Xinhui Yu[1] · Yaohui Lin[1] · Xusheng Wang[1] · Liangjun Xu[1] · Zongwen Wang[2] · FengFu Fu[1]

Received: 23 February 2018 / Accepted: 14 April 2018 / Published online: 21 April 2018

Abstract

An exonuclease-assisted multicolor aptasensor was developed for the visual detection of ochratoxin A (OTA). It is based on the etching of gold nanorods (AuNRs) mediated by a G-quadruplex-hemin DNAzyme. A DNA sequence (AG4-OTA) was designed that comprises a hemin aptamer and an OTA aptamer. OTA binds to AG4-OTA to form an antiparallel G-quadruplex, which halts its digestion by exonuclease I (Exo I) from the 3′-end of AG4-OTA. Thus, the retained hemin aptamer can bind to hemin to form a G-quadruplex-hemin DNAzyme. This DNAzyme has peroxidase-like activity that catalyzes the oxidation of 3,3′,5,5′-tetramethylbenzidine (TMB) by H_2O_2 to produce its diimine derivative (TMB^{2+}) in acidic solution. TMB^{2+} can etch the AuNRs by oxidizing Au(0) into Au(I). This results in the generation of rainbow-like colors and provides a multicolor platform for the visual detection of OTA. The assay is based on the use of a single isolated aptamer and possesses obvious advantages such as multi-color visual inspection, relatively high sensitivity and accuracy. It can be used to detect as little as 30 nM concentrations of OTA by visual observation and even 10 nM concentrations by spectrophotometry. The method was successfully applied to the determination of OTA in spiked beer where it gave recoveries of 101–108%, with a relative standard deviation (RSD, $n = 5$) of <5%.

Keywords Aptamer · Beer · Biosensor · Colorimetric detection · DNA · Mycotoxins · Biotoxin · Gold nanorods

Introduction

Ochratoxin A (OTA), a secondary metabolite of some fungi belonging to the genera *Aspergillus* and *penicillium (e.g. Penicillium verrucosum and Aspergillus ochraceus)*, can be present in foodstuff such as cereals, wine, coffee beans, nuts and animal feed [1, 2]. OTA represents a major risk to human and animal health due to its nephrotoxicity, immunotoxicity, genotoxicity, hepatotoxicity, and teratogenic toxicity [3]. General methods utilized for the detection of OTA include high performance liquid chromatography (HPLC), high performance liquid chromatography-mass spectrometry (HPLC-MS) and immunoassay [4–6]. However, these methods have obvious disadvantages, for example, HPLC and HPLC-MS require expensive equipment and time-consuming pretreatment, and immunoassay is limited by cross-reactively and poor shelf life of antibody. Hence, it is essential to develop a simple, cost-effective and instrument-free method for the on-site detection of OTA.

Aptamers are ssDNA or ssRNA sequences. They are typically isolated via *in vitro* systematic evolution of ligands by exponential enrichment (SELEX). They have gained considerable attention as good bio-recognition

Electronic supplementary material The online version of this article (https://doi.org/10.1007/s00604-018-2811-9) contains supplementary material, which is available to authorized users.

✉ Zongwen Wang
13067421373@163.com

✉ FengFu Fu
fengfu@fzu.edu.cn

[1] Key Laboratory for Analytical Science of Food Safety and Biology of MOE, Fujian Provincial Key Lab of Analysis and Detection for Food Safety, College of Chemistry, Fuzhou University, Fuzhou 350116, Fujian, China

[2] State Key Laboratory of Ecological Pest Control for Fujian and Taiwan Crops, College of Plant Protection, Fujian Agriculture and Forestry University, Fuzhou 350002, China

element for detection of different targets such as drugs, protein, and cell [7–9]. Unlike antibody, once the sequence of an aptamer was identified, it can be chemically synthesized and modified in an inexpensive manner with high reproducibility and long shelf life. Since OTA aptamer has been reported in 2008 [10], it has been widely employed to develop various methods including surface plasmon resonance, colorimetry, fluorometry, electroanalysis, and so on for the rapid detection of OTA [11–15]. The strategy of strand displacement has been widely used to make the conformational changes of aptamer upon OTA binding and therefore generate signal. However, this strategy requires the optimization of aptamer-complementary DNA sequence. Furthermore, the strand displacement strategy may inevitably reduce target-binding affinity, which will lead to the impairment of performance. In addition, the previous colorimetric methods for OTA are all based on the monochromic intensity changes, which seriously confine the accuracy of visual inspection.

G-quadruplex-hemin DNAzymes not only have horseradish peroxidase-like activity but also obvious advantages over protein enzymes, such as low cost and high stability against hydrolysis and heat treatment [16–19]. It has been widely used in some colorimetric methods to catalyze substrate for producing colored product. These colorimetric biosensors have some advantages, such as low cost, on-site applicability, no requirement of expensive instrument, and relatively short analysis time. However, most of previous colorimetric biosensors just present single color, which seriously confine the accuracy of visual inspection. Gold nanorods (AuNRs) attracted more and more attention because it has a broadly tunable aspect ratio (ratio of length to diameter) [20]. With various aspect ratios, AuNRs suspended in solution displayed a range of different colors and surface plasmon resonance (SPR) absorption. In view of above optical properties, some multicolor assays based on the etching of AuNRs have been developed for the visual determination of some targets such as glucose, antigen and ions [21–24]. This method is not only label-free, non-modification and non-aggregation, but also is able to perform visual detection with relatively better accuracy. With these facts in mind, we developed a multicolor biosensor to perform the visual detection of OTA by utilizing exonuclease I (Exo I) to differentiate the conformational change between OTA-bound and free aptamer, and using the catalytic product of 3,3′,5,5′-tetramethylbenzidine (TMB), its diimine derivative (TMB^{2+}), to etch AuNRs for generating multicolor signal. The success of the multicolor aptasensor provided a potential approach for the instrument-free and on-site visual detection of OTA in drink sample.

Materials and methods

Reagents

Exonuclease I (*E. coli*) and $RecJ_f$ were purchased from New England Biolabs (USA, https://international.neb.com/). SYBR Gold was purchased from Invitrogen (USA, https://www.thermofisher.com/cn/zh/home/brands/invitrogen.html). Ochratoxin A (OTA), ochratoxin B (OTB) and aflatoxins B1 (AFB1) were purchased from Fermentek Ltd. (Israel, http://fermentek.com/). $HAuCl_4$ was purchased from Aladdin (Shanghai, China, http://www.aladdin-e.com/). Cetyltrimethyl ammonium bromide (CTAB), TMB-H_2O_2 solution, and the other chemical reagents were purchased from Sigma-Aldrich (USA, https://www.sigmaaldrich.com/). All DNA were ordered from Sangon Biotech Co., Ltd. (Shanghai, China, http://www.sangon.com/) and dissolved in TE buffer (10 mM Tris, 1 mM EDTA, pH 7.5). DNA concentrations were measured using a NanoDrop 2000 spectrophotometer (Thermo Scientific, USA, https://www.thermofisher.com/). The DNA sequences were showed in Table S1 (see electronic supporting material, ESM). The probe AG4-OTA was a sequence combined hemin aptamer (AG4, bold at the 5′-end) and OTA aptamer (underline, at the 3′-end) with a linker of four adenosines. OTA-34 and OTA-33 were OTA aptamer lose first two and three nucleotides from 3′ end, respectively. The other buffer used in the experiment is as follow: reaction buffer (100 mM Tris, 500 mM $MgCl_2$, 100 mM NaCl, 1.0 mg/mL BSA, pH 7.5), and TES buffer (10 mM Tris, 1.0 mM EDTA, 2.2 M NaCl, 0.1 M KCl, pH 7.5).

Preparation of gold nanorods

The AuNRs solution was prepared according to the typical seed-mediated method [25]. Firstly, the seed solution was prepared in a glass vial (25 mL) by adding 0.6 mL of 0.01 M freshly prepared $NaBH_4$ solution to the mixture of 10 mL 0.1 M CTAB and 0.25 mL 0.01 M $HAuCl_4$ under vigorous stirring at 30 °C. After 2 min, the stirring was turned off and the seed solution was incubated at 30 °C for 2 h. The growth solution was prepared by adding ascorbic acid (0.32 mL, 0.1 M) into a solution containing $HAuCl_4$ (2 mL, 0.01 M), $AgNO_3$ (0.25 mL, 0.01 M), HCl (0.8 mL, 1 M) and CTAB (40 mL, 0.1 M). Finally, 96 μL of the seed solution was added into the 43.37 mL growth solution, and the mixture was vigorously stirred for 10 s and then matured for 24 h under static conditions at 30 °C. Then, 40 mL of the prepared AuNRs was concentrated to obtain AuNRs precipitate by centrifuging at 10000 rpm for 20 min, and the AuNRs precipitate was diluted to 40 mL with

water and then was concentrated again by centrifugation. Finally, the AuNRs precipitate was re-dispersed into 4 mL of CTAB solution (0.1 M) and stored in room temperature for next use. The prepared AuNRs has a ~55 nm length and ~14 nm diameter with a yellow color (see Fig. S1 in ESM). The concentration of the AuNRs solution was about 0.41 nM, as calculated according to an extinction coefficient of AuNRs at 740 nm of 4.0828×10^9 $M^{-1} \cdot cm^{-1}$ [26].

Colorimetric detection of OTA

All experiments were performed with the following process unless specified otherwise. Firstly, 1.2 μL of 50 μM AG4-OTA DNA solution and 6 μL of reaction buffer were added into 46.8 μL of OTA standard or sample solution, followed by adding 6 μL of Exonuclease I (Exo I, 2 U/μL) to perform digestion process at 23 °C. After 30 min digestion, 4 μL of 160 μM hemin solution, which was prepared in TES buffer, was added. Subsequently, the mixture solution was heated at 95 °C for 2 min to inactivate Exo I following by incubation at 30 °C for 10 min. After adding 16 μL of TMB-H_2O_2 solution, the whole solution was reacted for 30 min accompanying with color change from colorless to blue. Then, the reaction was stopped by adding 8 μL of 2 M H_2SO_4 to generate TMB diimine derivative (TMB^{2+}), which is bright yellow. Finally, 80 μL of above solution was gently mixed with AuNRs solution (5.4 μL of AuNRs stock solution diluted into 10.6 μL of 0.4 M CTAB solution). After reaction for 10 min, the color of solution was recorded by the camera, and the absorbance spectrum of solution was measured from 400 to 1000 nm by Tecan Spark 10 M microplate-reader (Tecan, Switzerland, https://www.tecan.com/). To evaluate the effect of experimental conditions on the etching AuNRs, the signal gain defined as $(\lambda_{OTA(+)} - \lambda_{OTA(-)})/(\lambda_{OTA(-)} - \lambda_{AuNRs})$ was calculated. In this formula, $\lambda_{OTA(+)}$ and $\lambda_{OTA(-)}$ present the maximal absorption wavelength of etched AuNRs solution in the presence and absence of OTA respectively, and λ_{AuNRs} presents the maximal absorption wavelength of AuNRs solution without etching. Higher signal gain means relatively bigger difference between $\lambda_{OTA(+)}$ and $\lambda_{OTA(-)}$, and relatively smaller difference between $\lambda_{OTA(-)}$ and λ_{AuNRs}.

Detection of OTA in beer samples

Firstly, beer was degassed in ultrasonicator for 5 min. Then, the OTA in beer samples was directly detected according to above process, and the data was compared with that obtained with standard method, HPLC-MS [27].

Results and discussion

Principle of multicolor detection

The detailed principle of multicolor detection is schematically illustrated in Scheme 1. The AG4-OTA DNA sequence, which combines hemin aptamer and OTA aptamer (at the 3′ end) with a linker of four adenosines, is used as probe. In the presence of OTA, AG4-OTA sequence bound to OTA to form an antiparallel G-quadruplex conformation. This antiparallel G-quadruplex conformation halts the Exo I digestion from the 3′ end of AG4-OTA, which results in the remaining of AG4 sequence (hemin aptamer). Upon the addition of hemin, hemin can bind with AG4 sequence to form G-quadruplex-hemin DNAzyme, which has peroxidase activity and can catalyze H_2O_2 to oxidize TMB into blue TMB^+. After adding with H_2SO_4, the H_2O_2-mediated oxidization of TMB was stopped and the resulting TMB^+ was oxidized to produce yellow TMB^{2+}. The TMB^{2+} can etch AuNRs to decrease the aspect ratios of AuNRs and thus generate color change. With the increasing of OTA concentration, the TMB^{2+} concentration increased, and as a result, the aspect ratios of AuNRs gradually decrease, which makes the solution display a colorful transition as shown in Scheme 1. Whereas, in the absence of OTA, the AG4-OTA sequence forms as random coil and thus can be totally digested into mononucleotides by Exo I. Hemin cannot bind with mononucleotides to form G-quadruplex-hemin DNAzyme, and thus were not able to catalyze H_2O_2-mediated oxidization of TMB to produce TMB^{2+} in acidic solution. So, AuNRs do not be etched and thus remain the original color. This provides a colorful sensing platform for the visual detection of OTA based on multicolor discrimination. The etching mechanism of AuNRs by TMB^{2+} has been reported in previous studies [28, 29]. In the present of CTAB, CTAB in the AuNRs solution can partly ionize into Br^- and CTA^+, and the released Br^- and CTA^+ can complex with Au(I) to form $[AuBr^{2-}$-$CTA^+]$/Au(0) redox electric pair, which has a redox potential <0.2 V (versus normal hydrogen electrode, NHE) [28]. The redox potential of TMB^{2+} is in the range of 0.22–0.7 V (versus NHE), therefore, the TMB^{2+} can effectively oxidize Au(0) into Au(I) in the present of CTAB and thus realize the etching of AuNRs [24].

To confirm the feasibility of our strategy, the digestion products of OTA aptamer were firstly characterized by 15% denaturing polyacrylamide gel electrophoresis (PAGE, details see electronic supporting material 1, ESM 1). Two exonucleases, Exo I and $RecJ_f$, which were reported can specifically degrades single-strand DNA form 3′ to 5′ and 5′ to 3′ respectively, were employed to digest OTA aptamer. As observed in Fig. 1a, in the absence of OTA, OTA aptamer was completely digested into mononucleotides by Exo I. Whereas, in the presence of OTA, OTA aptamer was

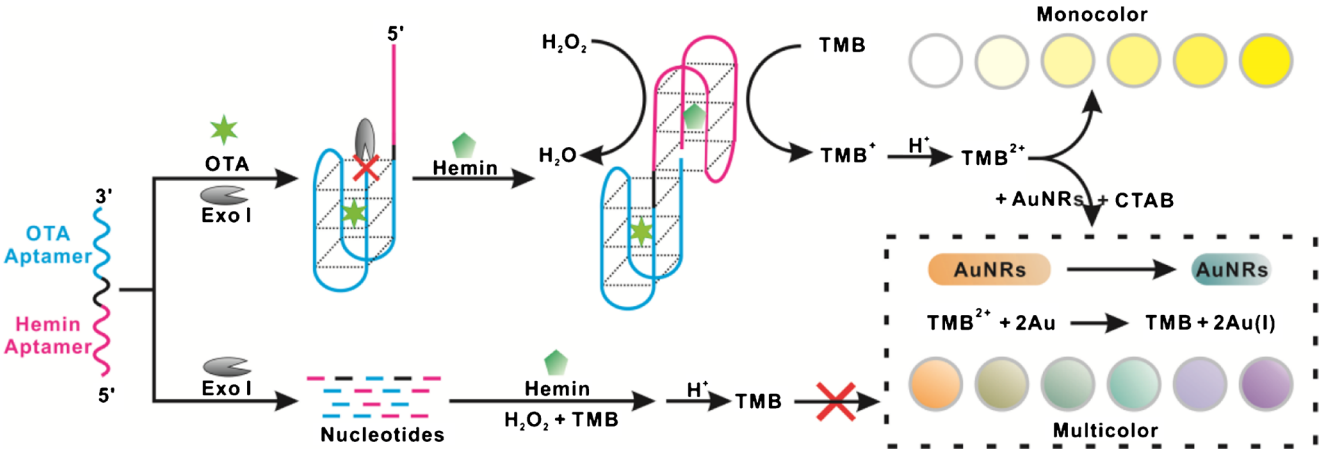

Scheme 1 The schematic illustration of the principle of exonuclease-assisted multicolor OTA detection

digested by Exo I to lose only two nucleotides to generate a 34-nt major product (OTA-34) after a 30-min reaction. This is because that OTA bind to OTA aptamer and OTA-34 to form antiparallel G-quadruplex, and thus inhibits Exo I digestion. To confirm whether the Exo I activity was inhibited by OTA-bound aptamer or by OTA itself, the random DNA, which is a single-strand DNA without binding affinity to OTA, was used to perform the same digestion reaction. As shown in Fig. 1b, no digestion inhibition was observed, indicating that OTA itself can not affect Exo I activity. The circular dichroism spectra also showed both OTA aptamer and OTA-34 can bind to OTA to form antiparallel G-quadruplex (Fig. 1e). These results indicated that the antiparallel G-quadruplex conformation formed by OTA-bound aptamer efficiently inhibited the Exo I digestion. For the $RecJ_f$ digestion experiment, the similar results were found that OTA-bound aptamer inhibited the $RecJ_f$ digestion in first nucleotide (Fig. 1c) and OTA was unable to affect $RecJ_f$ activity (Fig. 1d). By considering that the $RecJ_f$ digestion experiment must be performed at 37 °C and the price of $RecJ_f$ was more expensive than that of Exo I, Exo I was selected.

The morphology, color and SPR adsorption spectrum of AuNRs for detecting different concentrations of OTA were also investigated to further confirm the feasibility of our strategy. As results shown in Fig. 2, with the increasing of OTA concentration from 0 to 200 nM, the length of AuNRs decreased from ~55 nm to ~33 nm (the statistical distribution of AuNRs length was shown in Fig. S2 in ESM), and the color of solutions changed from yellow to blue. Correspondingly, the longitudinal peak shifted from 716 nm to 624 nm. All above results verified the feasibility of our strategy.

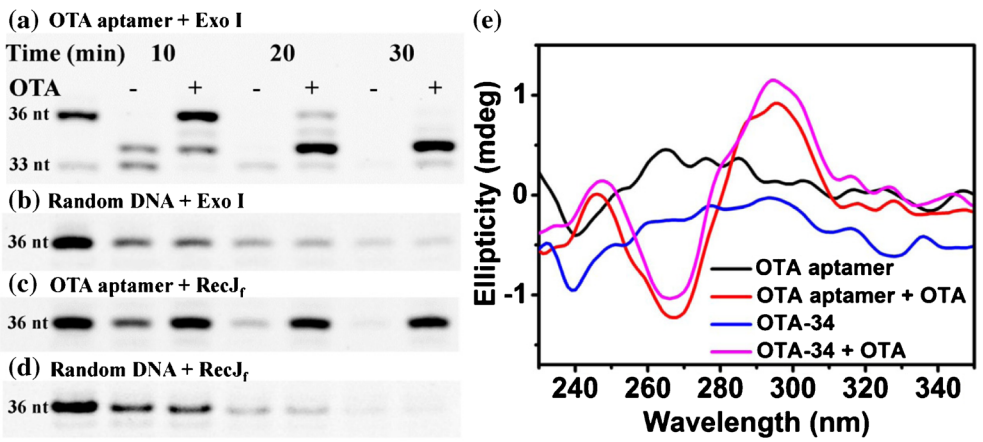

Fig. 1 Figure on the left: The PAGE of Exo I digestion products of OTA aptamer (**a**) and random DNA (**b**), and the PAGE of $RecJ_f$ digestion products of OTA aptamer (**c**) and random DNA (**d**). The symbols of "-" and "+" in figure represent the digestion solution in the absence and presence of OTA, respectively. Digestion temperature were 23 °C and 37 °C for the Exo I digestion and the $RecJ_f$ digestion, respectively. Other conditions: [DNA] = 1 μM, [$MgCl_2$] = 10 mM, [NaCl] = 50 mM, [OTA] = 2 μM, [Exo I] = 0.2 U/μL, [$RecJ_f$] = 0.5 U/μL. Figure on the right: The CD spectra (E) of OTA aptamer and OTA-34 in reaction buffer. Other conditions: [DNA] = 3 μM, [OTA] = 10 μM

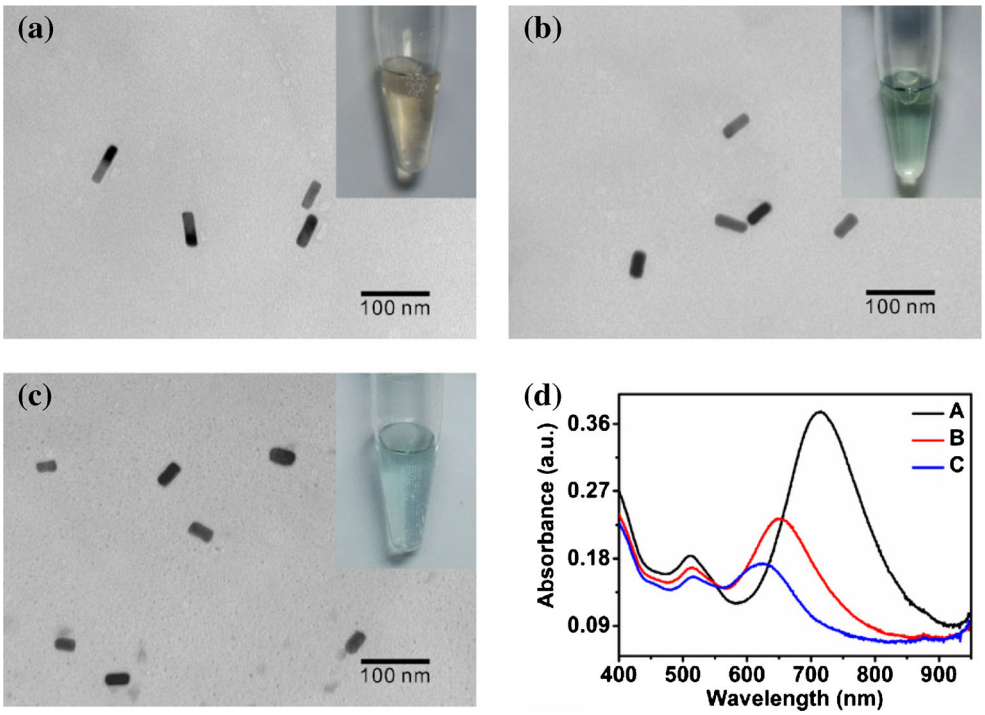

Fig. 2 The TEM images, photograph and UV-Visible absorption spectra of AuNRs solution for detecting 0 nM (**a**), 100 nM (**b**), and 200 nM (**c**) of OTA. Other conditions: [AG4-OTA] = 1 μM, [Exo I] = 0.2 U/μL, [hemin] = 10 μM, [TMB-H_2O_2] = 20 μL, [CTAB] = 50 mM

Optimization of Exo I digestion condition

The Exo I digestion of AG4-OTA is one of key considerations in this method. By considering that Na^+ can induce OTA aptamer to form antiparallel G-quadruplex structure [21], the effect of sodium ion and magnesium ion on the Exo I digestion reaction was investigated by a fluorescent experiment, which uses SYBR Gold as fluorescent signal (details see ESM 2). As observed in Fig. S3-A (see ESM), at a fixed Mg^{2+} concentration of 10 mM, the activities of Exo I were halted with the increasing of Na^+ concentration regardless of the presence of OTA, indicating more antiparallel G-quadruplex structures were formed in higher Na^+ concentration. The signal gain defined as $(F_{OTA(+)}\text{-}F_{OTA(-)})/F_{OTA(-)}$ was calculated, and the maximum value was obtained in 10 mM Na^+ solution (see Fig. S3-B in ESM). Mg^{2+} is necessary for the activity of Exo I [22]. At a fixed Na^+ concentration of 10 mM, the activities of Exo I obviously increased with the increasing of Mg^{2+} concentration in the absence of OTA, but only slightly increased in the presence of OTA (Fig. S3-C in ESM). The signal gain reached a platform when Mg^{2+} concentration was 50 mM (Fig. S3-D in ESM). Therefore, a final concentration of 10 mM Na^+ and 50 mM Mg^{2+} was selected.

Optimization of etching condition

The etching experimental conditions including concentration of hemin and CTAB, volume of TMB-H_2O_2 solution, and the reaction time of catalytic oxidation were optimized. The concentration of hemin and the volume of TMB-H_2O_2 solution directly affect the amount of produced TMB^{2+}, and thus affect the etching of AuNRs. Generally, in the presence of OTA, higher concentration of hemin and more volume of TMB-H_2O_2 solution will produce more amount of TMB^{2+} to effectively etch AuNRs, but higher TMB^{2+} concentration may bring higher background signal as well. The concentration of hemin was optimized in the range from 5 to 30 μM. As Fig. S4-A showed (see ESM), the signal gain defined as $(\lambda_{OTA(+)} - \lambda_{OTA(-)})/(\lambda_{OTA(-)} - \lambda_{AuNRs})$ showed an obvious correlativity with hemin concentration. The maximum value was obtained when the concentration of hemin was 10 μM, and thus 10 μM was selected as the optimal concentration of hemin. The volume of TMB-H_2O_2 solution was optimized in the range from 12 to 24 μL, and 20 μL was selected as the optimal volume of TMB-H_2O_2 solution (Fig. S4-B in ESM).

CTAB serves as the complexing agent in the oxidation reaction of AuNRs [30]. The concentration of CTAB was optimized in the range from 30 to 80 mM. The result (Fig. S4-C in ESM) showed that the characteristic peak of TMB^{2+} (452 nm) was reduce with increasing concentration of CTAB, indicating the etching reaction was more completely performed in higher CTAB concentration. However, when concentration of CTAB is higher than 50 mM, the longitudinal peak of AuNRs broadens and the peak value was a little redshift. This phenomenon may attribute to non-uniform etching of the AuNRs because the high CTAB concentration in AuNRs solution has higher viscosity that impedes rapid mixing of AuNRs solution and TMB^{2+} solution. So, 50 mM was selected as the optimal concentration of CTAB. Finally, the reaction time of catalytic oxidation of TMB was investigated. The result (Fig.

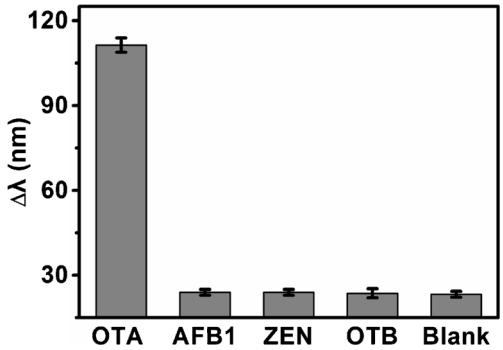

Fig. 3 The selectivity of the method. The concentrations of OTA, AFB1, ZEN and OTB are all 200 nM. Other conditions: [AG4-OTA] = 1 μM, [Exo I] = 0.2 U/μL, [hemin] = 10 μM, [TMB-H_2O_2] = 20 μL, [CTAB] = 50 mM

S4-D in ESM) showed that the signal gain increased with the increasing of reaction time when reaction time is less than 30 min. When the reaction time is more than 30 min, the signal gain was decrease since the background signal increased. Hence, 30 min was selected as optimal reaction time.

Specificity for OTA determination

To evaluate the selectivity, other mycotoxins including AFB1, ZEN, and OTB were chosen as the interferents. The longitudinal peak shift induced by OTA and interferents (200 nM) under the optimized conditions was compared. As Fig. 3 showed, compared with the blank, the longitudinal peak shift were negligible in the case of other mycotoxins. Whereas, a great longitudinal peak shift was observed in the case of OTA, indicating that the assay has a high selectivity for OTA.

Analytical performance of the method

Under the optimal conditions, various concentrations of OTA (10 nM - 2 μM) were tested. As shown in Fig. 4, a series of color from yellow to purple were observed in the solution while OTA concentration increased form 10 nM to 1.0 μM. The color change can be clearly identified by bare eye observation when the OTA concentration is 30 nM, *i.e.* the visual detection limits is 30 nM for OTA. Correspondingly, the UV-visible spectra of solutions showed that the longitudinal peak gradually shifted from 716 nm to 595 nm with the increasing of OTA concentration from 0.0 to 1.0 μM. The longitudinal peak shift (Δλ) had a linear correlation with the OTA concentration in the range of 10 to 200 nM. The method has a good repeatability with RSD < 5%, and the detection limit was calculated to be 10 nM by UV-visible spectrometry.

To demonstrate the potential application in real sample, the recovery rates were performed when four levels of concentration of OTA were spiked in beer samples. As results shown in Table 1, the spiked samples with different concentrations of OTA displayed different colors. For example, the spiked sample with 0.3 μM OTA displayed purple which was similar to the colors of standard samples with same OTA concentrations. Another spiked samples had the same situation. The Table 1 showed that the recovery rate was 101% to 108%, and RSD ($n = 5$) was smaller than 5%. The results were consistent with those obtained with HPLC-MS. It was reported that the OTA concentrations in beer may vary in the range of 7.5 to 5850 nM [31]. Hence, the method can be applied to visual measurement of

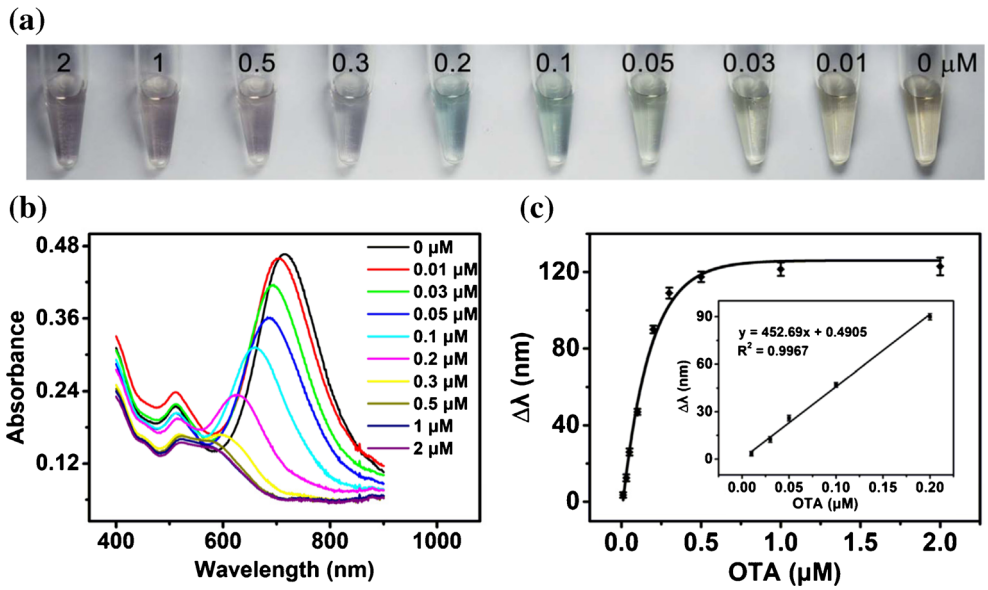

Fig. 4 The color change (**a**), UV-Visible spectra (**b**) and calibration curve (**c**) for detecting different concentration of OTA

Table 1 Analytical results of OTA in beer samples

Sample	OTA added (nM)	OTA detected				
		Bare eye observation (nM)	UV-visible spectrometry			HPLC-MS (nM)
			Concentration (nM)	RSD (n=5, %)	Recovery (%)	
1	300		~300	*N/A	*N/A	304.6
2	200		214.5	5%	107%	201.6
3	100		108.4	4%	108%	98.9
4	50		50.6	4%	101%	48.8

* Data was not obtained since the concentration of OTA is beyond the linear range

OTA in real beer sample with satisfied accuracy and sensitivity.

So far, most of colorimetric methods for the detection of OTA were based on the monochromic intensity changes [12, 32–35]. Compared to previous methods (see Table S2 in ESM), the colorimetric method showed multiple colors, which was more easily and accurately distinguished by bare eyes observation without any instrument, corresponding to different OTA concentration. In addition, the method has relatively low visual detection limit and short analysis time. Hence, the colorimetric method provided a potential alternative for the instrument-free and on-site visual detection of OTA in drink sample.

Conclusions

In summary, a multicolor bioassay for the visual detection of OTA based on the Exo I digestion of aptamer and G-quadruplex-hemin DNAzyme-mediated etching of the AuNRs was developed. AG4-OTA DNA sequence, which is a signal-strand DNA combined hemin aptamer (AG4) and OTA aptamer with a linker of four adenosines, was designed as recognition probe. In the presence of OTA, OTA-bound AG4-OTA halted the Exo I digestion and thus retaining complete AG4 sequence. The retaining AG4 sequence can bind with hemin to form G-quadruplex-hemin DNAzyme, which possesses peroxidase activity and can effectively catalyze the H_2O_2-mediated oxidization of TMB to product TMB^{2+} in

acidic solution. The obtained TMB^{2+} can effectively etch AuNRs to alter the aspect ratios of AuNRs, which makes the solution display a colorful transition. This provided a platform for fabricating multicolor OTA bioassay. It can be used to detect as little as 30 nM of OTA concentration by bare eye observation and 10 nM of OTA concentration by UV-visible spectrophotometry. The biosensor was successfully applied to detect OTA in beer sample with a recovery of 101–108% and a RSD ($n = 5$) < 5%. The success in the present study provided a label-free and low-cost method for the instrument-free and on-site visual detection of OTA in drink sample.

Acknowledgements We gratefully acknowledge the National Key Research and Development Program of China (2017YFC1600500), NSFC (21505020, 21677034) and the Program for Changjiang Scholars and Innovative Research Team in University (No. IRT-15R11) for financial support.

Compliance with ethical standards The author(s) declare that they have no competing interests.

References

1. Amézqueta S, González-Peñas E, Murillo-Arbizu M, de Cerain AL (2009) Ochratoxin A decontamination: A review. Food Control 20: 326–333
2. Malir F, Ostry V, Novotna E (2013) Toxicity of the mycotoxin ochratoxin A in the light of recent data. Toxin Rev 32:19–33
3. Sorrenti V, Giacomo CD, Acquaviva R, Barbagallo I, Bognanno M, Galvano F (2013) Toxicity of ochratoxin A and its modulation by antioxidants: a review. Toxins 5:1742–1766
4. Pena A, Cerejo F, Lino C, Silveira I (2005) Determination of ochratoxin A in Portuguese rice samples by high performance liquid chromatography with fluorescence detection. Anal Bioanal Chem 382:1288–1293
5. Solfrizzo M, Gambacorta L, Lattanzio VM, Powers S, Visconti A (2011) Simultaneous LC–MS/MS determination of aflatoxin M1, ochratoxin A, deoxynivalenol, de-epoxydeoxynivalenol, α and β-zearalenols and fumonisin B1 in urine as a multi-biomarker method to assess exposure to mycotoxins. Anal Bioanal Chem 401:2831–2841
6. Adányi N, Levkovets I, Rodriguez-Gil S, Ronald A, Váradi M, Szendrő I (2007) Development of immunosensor based on OWLS technique for determining Aflatoxin B1 and Ochratoxin A. Biosens Bioelectron 22:797–802
7. Fang X, Tan W (2010) Aptamers generated from cell-SELEX for molecular medicine: a chemical biology approach. Acc Chem Res 43:48–57
8. Strehlitz B, Nikolaus N, Stoltenburg R (2008) Protein detection with aptamer biosensors. Sensors 8:4296–4307
9. Cerchia L, De Franciscis V (2010) Targeting cancer cells with nucleic acid aptamers. Trends Biotechnol 28:517–525
10. Cruz-Aguado JA, Penner G (2008) Determination of ochratoxin A with a DNA aptamer. J Agric Food Chem 56:10456–10461
11. Bianco M, Sonato A, De Girolamo A, Pascale M, Romanato F, Rinaldi R, Arima V (2017) An aptamer-based SPR-polarization platform for high sensitive OTA detection. Sensors Actuators B Chem 241:314–320
12. Wang C, Qian J, Wang K, Yang X, Liu Q, Hao N, Wang C, Dong X, Huang X (2016) Colorimetric aptasensing of ochratoxin A using Au@ Fe 3 O 4 nanoparticles as signal indicator and magnetic separator. Biosens Bioelectron 77:1183–1191
13. Wang C, Qian J, An K, Huang X, Zhao L, Liu Q, Hao N, Wang K (2017) Magneto-controlled aptasensor for simultaneous electrochemical detection of dual mycotoxins in maize using metal sulfide quantum dots coated silica as labels. Biosens Bioelectron 89:802–809
14. Wang S, Zhang Y, Pang G, Zhang Y, Guo S (2017) Tuning the aggregation/disaggregation behavior of graphene quantum dots by structure-switching aptamer for high-sensitivity fluorescent Ochratoxin A sensor. Anal Chem 89:1704–1709
15. Wu H, Liu R, Kang X, Lian C, Lv L, Guo Z (2018) Fluorometric aptamer assay for ochratoxin A based on the use of single walled carbon nanohorns and exonuclease III-aided amplification. Microchim Acta 185:27
16. Zhang D, Wang W, Dong Q, Huang Y, Wen D, Mu Y, Yuan Y (2018) Colorimetric detection of genetically modified organisms based on exonuclease III -assisted target recycling and hemin/G-quadruplex DNAzyme amplification. Microchim Acta 185:75
17. Sang Y, Xu Y, Xu L, Cheng W, Li X, Wu J (2017) Colorimetric and visual determination of micro RNA via cycling signal amplification using T7 exonuclease. Microchim Acta 184:2465–2471
18. Nasir M, Nawaz MH, Latif U, Yaqub M, Hayat A, Rahim A (2017) An overview on enzyme-mimicking nanomaterials for use in electrochemical and optical assays. Microchim Acta 184:323–342
19. Zong C, Zhang D, Yang H, Wang S, Chu M, Li P (2017) Chemiluminescence immunoassay for cardiac troponin T by using silver nanoparticles functionalized with hemin/G-quadruplex DNAzyme on a glass chip array. Microchim Acta 184:3197–3204
20. Ye X, Jin L, Caglayan H, Chen J, Xing G, Zheng C, Doan-Nguyen V, Kang Y, Engheta N, Kagan CR (2012) Improved size-tunable synthesis of monodisperse gold nanorods through the use of aromatic additives. ACS Nano 6:2804–2817
21. Lin Y, Zhao M, Guo Y, Ma X, Luo F, Guo L, Qiu B, Chen G, Lin Z (2016) Multicolor colormetric biosensor for the determination of glucose based on the etching of gold nanorods. Sci Rep 6:37879
22. Zhang Z, Chen Z, Cheng F, Zhang Y, Chen L (2017) Highly sensitive on-site detection of glucose in human urine with naked eye based on enzymatic-like reaction mediated etching of gold nanorods. Biosens Bioelectron 89:932–936
23. Chen Z, Liu R, Wang S, Qu C, Chen L, Wang Z (2013) Colorimetric sensing of copper (II) based on catalytic etching of gold nanorods. RSC Adv 3:13318–13323
24. Ma X, Lin Y, Guo L, Qiu B, Chen G, Yang HH, Lin Z (2017) A universal multicolor immunosensor for semiquantitative visual detection of biomarkers with the naked eyes. Biosens Bioelectron 87: 122–128
25. Nikoobakht B, El-sayed MA (2003) Preparation and growth mechanism of gold nanorods (NRs) using seed-mediated growth method. Chem Mater 15:1957–1962
26. Orendorff CJ, Murphy CJ (2006) Quantitation of metal content in the silver-assisted growth of gold nanorods. J Phys Chem B 110: 3990–3994
27. Beltran E, Ibáñez M, Sancho JV, Hernandez F (2009) Determination of mycotoxins in different food commodities by ultra-high-pressure liquid chromatography coupled to triple quadrupole mass spectrometry. Rapid Commun Mass Spectrom 23:1801–1809
28. Rodríguez-Fernández J, Pérez-Juste J, Mulvaney P, Liz-Marzán LM (2005) Spatially-directed oxidation of gold nanoparticles by Au(III)-CTAB complexes. J Phys Chem B 109:14257–14261

29. Cao GX, Wu XM, Dong YM, Li ZJ, Wang GL (2016) Colorimetric determination of melamine based on the reversal of the mercury(II) induced inhibition of the light-triggered oxidase-like activity of gold nanoclusters. Microchim Acta 183:441–448
30. Tsung CK, Kou X, Shi Q, Zhang J, Yeung MH, Wang JF, Stucky GD (2006) Selective shortening of single-crystalline gold nanorods by mild oxidation. J Am Chem Soc 128:5352–5353
31. Odhav B, Naicker V (2002) Mycotoxins in South African traditionally brewed beers. Food Addit Contam 19:55–61
32. Lin C, Zheng H, Sun M, Guo Y, Luo F, Guo L, Qiu B, Lin Z, Chen G (2018) Highly sensitive colorimetric aptasensor for ochratoxin A detection based on enzyme-encapsulated liposome. Anal Chim Acta 1002:90–96
33. Wang C, Dong X, Liu Q, Wang K (2015) Label-free colorimetric aptasensor for sensitive detection of ochratoxin A utilizing hybridization chain reaction. Anal Chim Acta 860:83–88
34. Yang C, Lates V, Prieto-Simón B, Marty JL, Yang X (2012) Aptamer-DNAzyme hairpins for biosensing of Ochratoxin A. Biosens Bioelectron 32:208–212
35. Yang C, Lates V, Prieto-Simón B, Marty JL, Yang X (2013) Rapid high-throughput analysis of ochratoxin A by the self-assembly of DNAzyme–aptamer conjugates in wine. Talanta 116:520–526